

AXIAL ALIGNMENT IN A RING-COLLECTION  
BETA-RAY SPECTROMETER

by

ERIC DAVIS EARLE

B.Sc., Memorial University of Newfoundland, 1958

A THESIS SUBMITTED IN PARTIAL FULFILMENT OF  
THE REQUIREMENTS FOR THE DEGREE OF

MASTER OF SCIENCE

in the Department  
of  
PHYSICS

We accept this thesis as conforming to the  
required standard

THE UNIVERSITY OF BRITISH COLUMBIA

August, 1960

In presenting this thesis in partial fulfilment of the requirements for an advanced degree at the University of British Columbia, I agree that the Library shall make it freely available for reference and study. I further agree that permission for extensive copying of this thesis for scholarly purposes may be granted by the Head of my Department or by his representatives. It is understood that copying or publication of this thesis for financial gain shall not be allowed without my written permission.

Department of Physics  
The University of British Columbia,  
Vancouver 8, Canada.  
Date Aug 9<sup>th</sup>/1960

ABSTRACT

A thin-lens beta-ray spectrometer using ring-focus collection was modified. These modifications consisted of; 1) a centering mechanism enabling the source-detector axis to be aligned with the magnetic axis; 2) an extension of the vacuum chamber placing the detector further from the magnet coils. The latter considerably decreased the magnetic shielding requirements for the detector. A misalignment of 0.25 mm. for parallel axes and of  $0^{\circ}09'$  for intersecting axes produced noticeably poorer performance. Using a gathering power of .70%, a resolving power of .94% was obtained for the 661.6 Kev. K-conversion peak of  $\text{Cs}^{137}$ .

# TABLE OF CONTENTS

	PAGE
I INTRODUCTION	
A. Nuclear Spectroscopy	1
B. Basic Ideas on Beta- and Gamma-Decay	3
C. Early Spectrometers and their Characteristics	13
II THE DEVELOPMENT OF THE THIN-LENS SPECTROMETER	21
III PRESENT INVESTIGATION	
A. Instrumentation	27
B. Experimental Tests	34
C. Conclusions	41
BIBLIOGRAPHY	45

## TABLE OF ILLUSTRATIONS

Figure	Following Page
1a.) 1b.) Typical Decay Schemes	4
2. Typical Beta-Ray Spectrum	4
3. Helical Spectrometer Electron Trajectories	16
4. Unmodified Thin-Lens Spectrometer	16
5. Detector Assembly of Mann and Payne	22
6. Modified Thin-Lens Spectrometer	23
7. Spectrometer Assembly	27
8. The Source Assembly	27
9. The Detector Assembly	28
10. Sample Entrance Baffle	30
11. Chamber Support	31
12. Variation of Peak Shape with Chamber Position	38
13. Some Sample Conversion Peaks	40

ACKNOWLEDGEMENTS

The work described in this thesis was supported by a Fund-in-Aid-of-Research to Dr. K.C. Mann by the National Research Council of Canada.

The author wishes to thank Dr. K.C. Mann for his able guidance and assistance throughout the course of this work.

Also the author thanks the National Research Council of Canada for awarding him a Bursary and Studentship for the period June 1958 to August 1960.

He wishes to express his appreciation to H.R. Schneider and F.A. Payne for helpful suggestions and criticisms and to F.J. Morgan for his assistance in the experimental work.

## I. INTRODUCTION

### A. NUCLEAR SPECTROSCOPY

It has been experimentally evident for some time that matter is composed of atoms. These atoms are minute particles and consist of a combination of a number of other, more fundamental particles. The number and arrangement of these fundamental particles determine the properties of any particular atom and, generally, make it distinguishable from other atoms with a different number and/or arrangement of fundamental particles. Basically, atoms consist of a heavy, positively charged core, called the nucleus, around which negatively charged particles, called electrons, "orbit". Nuclear physics is the study of the characteristics of the nucleus. The purpose of nuclear spectroscopy is to establish some of these characteristics.

To a first approximation, the nucleus is composed of two kinds of particles called nucleons, a positively charged particle called the proton and a neutral particle, the neutron. The number of protons,  $Z$ , the number of neutrons,  $N$ , their motions and interactions determine the nuclear characteristics.

Nuclei may be stable or unstable. The unstable ones are termed radioactive and decay to states of lower energy usually through the emission of radiation of some kind. A particular nucleus may exist in any one of several nucleonic configurations,

each with its characteristic energy. The lowest energy level is called the ground state and any nucleus in a higher energy state may decay to this ground state by the emission of energy in the form of electromagnetic radiation (photons or gamma-rays). A radioactive nucleus may also decay by particle emission, where energy is removed kinetically. Generally, during particle emission, the number of neutrons or the number of protons in the original or parent nucleus changes, thereby producing a new or daughter nucleus. In the low energy region the predominant modes of radioactive decay are gamma-ray emission and beta-particle emission. The beta-particles may be negatively charged (the negatron, experimentally identical with the atomic electron<sup>1</sup>) or positively charged (the positron).

The function of the nuclear spectrometer is to study the energy of the beta-particles and gamma-rays emitted during radioactive decay in the low energy region and to use the experimental data obtained to give information concerning the angular momentum (spin), the energy levels and the parity\* of the nuclear states involved in the decay. It is hoped that this data with data collected in other branches of nuclear physics will enable physicists to construct a theory capable of explaining and predicting nuclear phenomena.

---

\* Parity arises from the wave mechanical considerations of the reflection properties of the spacial part of solutions of the wave equation.



## B. BASIC IDEAS ON BETA- AND GAMMA-DECAY

A brief summary of present nuclear theory, in particular beta-decay and "internal conversion" theory, consistent with the experimental evidence collected to date is given below.

The types of decay of particular interest are:

1) Beta-particle decay; an unstable nucleus emits a negatron or positron. The parent nucleus containing  $Z$  protons and  $N$  neutrons decays to a daughter nucleus containing  $Z \pm 1$  protons and  $N \mp 1$  neutrons. The nucleus may also reach a lower energy state by the capture of an orbital electron, leading to the formation of the same nucleus as is reached by positron decay. This is called orbital electron capture.

2) Gamma-ray emission; an unstable or excited nucleus spontaneously emits electromagnetic radiation and drops to a lower energy state of the same nucleus. The energy ( $h\nu$ ) of the gamma-ray equals the energy difference of the states involved. ( $h$  - Plank's universal constant.  $\nu$  - the frequency of the emitted gamma-ray.) The lower energy state may or may not be the ground state of the nucleus. In the event that it is not, subsequent decays will occur until this state is reached. An alternative method of de-excitation may occur when the excitation energy is transferred to an orbital electron. The orbital electron escapes from the atom with an energy equal to  $h\nu - E_b$  where  $E_b$  is the binding energy of the atomic electron to the nucleus. This last mode of decay is called

### "Internal Conversion".

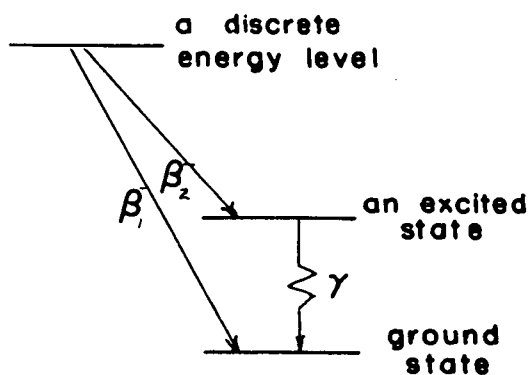
In general, a decay scheme consists of a combination of these modes of decay and often may be quite complex. Two decay schemes are shown in Figure 1. Here  $\beta_1^-$  and  $\beta_2^-$  represent beta-particle emission and  $\gamma$  represents electromagnetic radiation which may or may not be accompanied by internal conversion.

### Beta-decay.

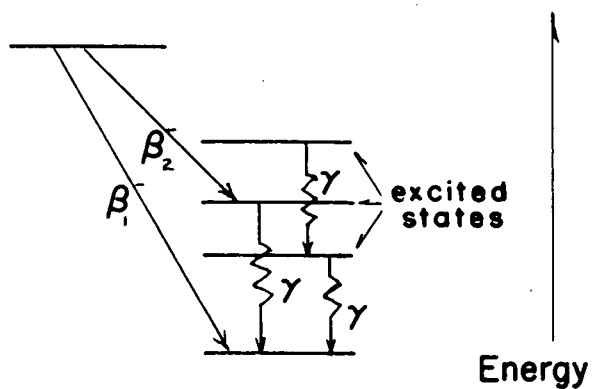
Nuclei with the same mass number, i.e.  $A = N + Z$ , are called isobars. Members of an isobaric group differ in  $Z$  (and  $N$ ) and in their actual nuclear masses. All beta-decays occur between members of the same isobaric group; in negatron emission the nuclear charge is increased by one positive unit; in positron emission or orbital electron capture the nuclear charge is decreased by one positive unit. To decide if some mode of particle decay is energetically possible one must consider the masses of parent, daughter and emitted particle. Let "a" represent a parent nucleus, "b" and "c" represent the product of its decay. Then decay will occur only if  $M(a) > M(b) + M(c)$  where  $M(x)$  represents the nuclear mass of the x particle. The excess mass  $m = M(a) - M(b) - M(c)$  is accounted for by the extra kinetic energy of the two product particles, using Einstein's energy equation  $E = m c^2$ .

Considering the atomic mass  $M_{at.}(Z, A)$  as distinct from the nuclear mass  $M(Z, A)$  we see that the above types of decay are energetically possible if:

PARENT      DAUGHTER  
 Z protons    Z+1 protons  
 N neutrons   N-1 neutrons



PARENT      DAUGHTER



Figs. 1a & 1b. Typical Decay Schemes

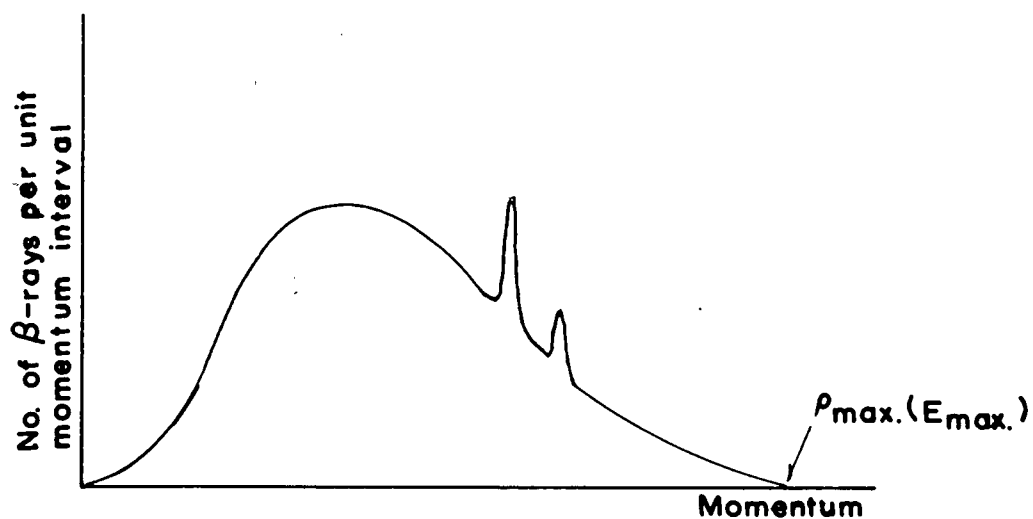


Fig. 2. Typical Beta-Ray Spectrum

$$M_{\text{at.}}(Z, A) > M_{\text{at.}}(Z + 1, A) \quad \text{for negatron decay}$$

$$M_{\text{at.}}(Z, A) > M_{\text{at.}}(Z - 1, A) + 2 M_0 \quad \text{for positron decay}$$

$$M_{\text{at.}}(Z, A) > M_{\text{at.}}(Z - 1, A) \quad \text{for orbital electron capture}$$

where  $M_0$  is the rest mass of the electron.

Orbital electron capture produces the same daughter nucleus as positron emission. It usually occurs in decays where positron emission is present and, because the mass requirements are not so severe, it sometimes occurs where positron emission is impossible.

For any group of isobaric nuclei the higher mass members always tend to decay to those of lower mass. For isobaric groups of odd  $A$  there exists only one stable member which is the end product to which all other isobaric members decay. However, for even  $A$  nuclei there may exist two or more stable nuclei in the same isobaric group. This is because the mass of even  $Z$ , even  $N$  nuclei is often less than the mass of either of its two odd-odd neighbours and so, if a lower mass state exists, the even-even nuclei can only reach it by double beta-decay. Ingrahm and Reynolds showed that the half life period for double beta-decay of  $\text{Te}^{130}$  is  $1.2 \times 10^{21}$  years, so that if this process occurs, it is very infrequent.

The decay scheme (Fig. 1) suggests that the beta-particles are emitted with discrete energies. One would expect, if number of beta-particles emitted per unit time were plotted

as a function of energy (or momentum), that only at certain energies would beta-particles be observed and these would correspond to the energy differences between the initial and final states. Such is not the case, however. Experimental evidence shows that the beta-energy spectrum is a continuous distribution, up to some end point energy (referred to as  $E_{\text{max.}}$ ). Frequently, spectral "lines" or peaks (Fig. 2) are superimposed on the continuum. These peaks are due to the internal conversion electrons. The continuous energy distribution, on the other hand, poses a dilemma, not easily resolved if one accepts the assumption that nuclear energy states are fixed, since fixed energy states would suggest a "line" structure for the primary beta-decay as well. The law of conservation of energy appears to be violated.

From a consideration of the angular momenta involved in the decay, i.e. the spins of the initial and final states and of the electron, it appears that the law of conservation of angular momentum is also violated. Finally, it may be shown that "statistics" are not conserved if only the beta-particle is involved in the decay.

These three difficulties, i.e. the energy continuum, angular momentum and statistics, may all be overcome if one accepts Pauli's suggestion that the beta-decay process involves the simultaneous emission of two particles -- the electron and the neutrino. The neutrino is postulated to be a new fundamental particle with no charge, very small mass

(probably zero), spin equal to  $\frac{1}{2}\hbar$  and which obeys Fermi-Dirac statistics. The existence of the neutrino now seems to be confirmed, experimentally.

In this concept the energy of the decay is shared between the two particles. According to the theory of the process worked out by Fermi, the beta-particle's energy distribution may be expressed by

$$P(E)dE \propto F(Z,E)p^2(E_{\max} - E)^2dE \quad (1)$$

where  $P(E)dE$  is the fraction of disintegrations which emit beta-particles with energy between  $E$  and  $E + dE$

$E_{\max}$  is the maximum energy observed in the spectrum

$E$  is the energy of the beta-particle

$p$  is the momentum of the beta-particle

$F(Z,E)$  is a complicated function which describes the effect of the Coulomb field of the nucleus on the emitted beta-particles.

From Equation (1) we see that  $\sqrt{\frac{N(p)}{p^2F}} \propto (E_{\max} - E)$  where  $N(p)$  is the number of beta-particles emitted with momentum  $p$ . Hence, if we plot  $\sqrt{\frac{N(p)}{p^2F}}$  as a function of  $E$  we get a straight line intersecting the energy axis at  $E_{\max}$ . This is called a Fermi plot. If other independent beta-groups are present in the spectrum then the end point energies of these groups may be obtained by subtracting successive contributions from the

composite Fermi plot.

Equation (1) is based on the assumption that the spin change ( $\Delta I$ ) is  $\pm 1, 0$  and that there is no parity change. This is the most probable mode of beta-decay and is called an "allowed" transition. All other transitions are called "forbidden", the degree of forbiddenness depending on the value of  $\Delta I$  and the presence or absence of parity change. Equation (1) gives a straight line plot only during allowed transitions.

For forbidden transitions, involving higher spin changes and possible parity changes, the "constant" in equation (1) becomes energy dependent and so gives a non-linear Fermi plot. Certain correction terms have been worked out and by applying these, it is possible to determine the degree of forbiddenness of the decay in question.

If  $P(E)dE$  represents the probability of beta-emission in the energy interval  $(E, E + dE)$  then the probability,  $\lambda$ , that the nucleus will decay by the emission of an electron in a particular beta group is:

$$\lambda = \int_0^{E_{max.}} P(E)dE.$$

This  $\lambda$  may be said to equal  $af$  where "a" is a constant and "f" is some function of  $Z$  and  $E$ . This total decay probability,  $\lambda$ , has dimensions disintegrations/time. Hence  $1/\lambda$  is the mean life ( $\tau$ ) of the excited particle. It can be shown that the mean life,  $\tau$ , and the half life,  $T_{\frac{1}{2}}$ , are re-

lated by

$$\tau = \frac{T_{\frac{1}{2}}}{\ln 2} = \frac{1}{\lambda} = \frac{1}{af}.$$

The quantity  $fT_{\frac{1}{2}}$  is called the comparative half-life of the transition. The logarithm of  $fT_{\frac{1}{2}}$  has been found convenient to work with in the comparison of beta-decay groups and is a useful way of indicating the degree of forbiddenness and hence spin and parity changes of the decay.

#### Gamma-decay.

As has been stated, a nucleus in an excited state may decay spontaneously to a lower state of the same nucleus by the emission of a gamma-ray. The energy of this gamma-ray is given by:

$$h\nu = E_2 - E_1$$

where  $E_2$ ,  $E_1$  are the energies of the upper and lower energy states.

The nucleus may also decay to this lower energy state by giving this energy to an electron in the K, L, ... shell of the same atom. The electron is then ejected with energy  $h\nu - E_K$ ,  $h\nu - E_L$ , ... where  $E_K$ ,  $E_L$ , ... are the binding energies of the orbital electrons.

This last de-excitation process is called internal conversion and the ejected electrons, conversion electrons.



These conversion electrons are emitted at discrete energies and will appear in a beta-energy spectrum as sharp peaks or conversion lines (Fig. 2). Those electrons in the innermost shell will have the greatest interaction probability with the nucleus. Thus the K-conversion line, usually, will be more intense than the L line, and so on.

The total probability,  $\lambda$ , that an excited nucleus will decay depends on the probability of gamma-emission,  $\lambda_\gamma$ , and the probability of internal conversion,  $\lambda_e$ . The probability of internal conversion may be broken down into probabilities of K conversion, L conversion, etc. Thus

$$\lambda = \lambda_\gamma + \lambda_e = \lambda_\gamma + \lambda_K + \lambda_L + \dots$$

The ratio of the number of decays by internal conversion to the number of decays by gamma-emission is called the conversion coefficient and is given by

$$\alpha = \frac{\lambda_e}{\lambda_\gamma} = \frac{\lambda_K}{\lambda_\gamma} + \frac{\lambda_L}{\lambda_\gamma} + \dots = \alpha_K + \alpha_L + \dots$$

where  $\alpha_K$ ,  $\alpha_L$ , ... are K, L, ... conversion coefficients.

To determine these coefficients experimentally, it is necessary to compare the relative intensities of the different modes of decay.

While the intensity of internally converted gamma-rays can be measured by the use of a beta-ray spectrometer, the intensity of gamma-rays cannot be measured directly. However,

if the gamma-rays are allowed to strike a foil, of high Z material, placed near the source, they will undergo a process called external conversion or a photoelectric process. In this process the energy of the gamma-ray is transferred to an orbital electron in the foil (or target) and the electron is then ejected with an energy equal to that of the gamma-ray less the binding energy of the orbital electron. Electrons ejected in this manner are called photo-electrons and may be analysed in the spectrometer. The foil, as a source of photo-electrons, becomes the source as seen by the spectrometer.

One might thus expect that a comparison of intensity measurements on internally and externally converted electrons would give sufficient information to determine experimentally the conversion coefficients. As theory predicts that these coefficients are functions of certain nuclear characteristics, the experimental evaluation of these coefficients would give valuable information on the spins and parities of the nuclear energy states.

Unfortunately, because of the lack of detailed knowledge of the photo-electric cross-section of the target in the low energy region where the internal conversion process predominates and because of the variation of the angle of emission of the photo-electrons with energy, one cannot use the external conversion spectrum for reliable comparison with the internal conversion spectrum. All one can do is compare photo-electron intensities of gamma-rays whose energies are

not too different.

However, the spectrometer may be used for a comparison of K, L, M, ... internal conversion intensities for any one transition. Values of these ratios,  $\frac{\alpha_K}{\alpha_L}$ ,  $\frac{\alpha_K}{\alpha_M}$ , ..., for various Z values, have been tabulated<sup>2</sup>. A comparison of measured and theoretical values of these ratios may give information concerning the nuclear states involved.

As illustrated in Figure 1a, nuclear states may decay by the emission of a gamma-ray or conversion electron. Frequently, many energy states are involved and the nucleus may emit multiple beta- and gamma-rays (Fig. 1b). In the majority of cases, excited nuclear states decay to lower states very quickly, for all practical purposes instantaneously. Relatively few nuclear states have lifetimes greater than  $10^{-10}$  secs. Such states are called isomeric states<sup>3,4</sup> and this designation merely means that the lifetime can be measured with techniques now available. These "cascade" decays are referred to as gamma-gamma-coincident decays.

Analysis of these cascade decays, of beta-gamma-decays and of the angular correlation between the beta- and gamma-rays or between two gamma-rays in cascade are useful in determining spin and parity changes and sometimes these analyses are performed with the aid of a spectrometer.

### C. EARLY SPECTROMETERS AND THEIR CHARACTERISTICS

As we have shown, measurements on nuclear transitions are important in the development of a consistent nuclear theory. These measurements may be obtained by the use of various instruments. In particular, spectrometers are used for measurements on internal and external conversion electrons, primary beta-particles and for coincidence and angular correlation work. These processes can only be studied properly if reasonably accurate energy and intensity measurements of the conversion electron lines and of the primary beta-groups can be obtained. This is the function of the beta-ray spectrometer.

Beta-ray spectrometers may employ electrostatic or magnetic focussing. The electrostatic spectrometer is energy selective while the, more generally used, magnetic spectrometer is momentum selective.

The electron trajectories in the magnetic spectrometers are determined by the momentum of the electron and the magnetic field such that

$$B e v = \frac{mv^2}{\rho}$$

where  $B$  is the component of the magnetic field normal to the particle's direction of motion

$e, m, v$  are the electron's charge, relativistic mass and velocity

$\rho$  is the radius of curvature of the electron's path.

The magnetic stiffness,  $B\rho$ , is normally used as the abscissa in plotting an electron spectrum and is proportional to the electron momentum (mv).

A spectrometer's two most important characteristics are its transmission (% collected) and its resolving power. These will be discussed in more detail later. In practice, the obtaining of ideal transmission and resolving power is limited by electron optical aberrations, source size, detector background, field form, power consumption and cooling, flexibility and economy, accurate adjustments (e.g. alignment), etc. A variety of spectrometers have been designed to minimize different combinations of these limitations and often are designed for analysis in either the low energy or high energy regions. For example, electrostatic spectrometers can economically and practically be used only in the low energy region, a field of 300,000 volts/cm. producing the same radius of curvature as a field of 1000 gauss.

Magnetic spectrometers may be divided into two groups, flat and helical. In the flat spectrometers the magnetic lines of force are mainly in a direction normal to the electron's path while in the helical spectrometers the lines of force are mainly in the direction of the electron's path.

The first determinations of beta-particle energy by their deflection in a magnetic field were carried out by von Baeyer and Hahn<sup>5</sup> by the "direct deflection method". Beta-rays emitted from a radioactive source were allowed to pass through a narrow

slit and then, after travelling an arbitrary distance through a magnetic field, were recorded on a photographic plate. Only crude measurements of intensity were possible since no attempt was made to focus the beta-rays.

The first magnetic focussing device, the semi-circular focussing spectrometer, soon followed, after a suggestion by Danysz<sup>6</sup>. It is based on the geometric fact that if two circles with the same radius are drawn with their centres separated by a small distance with respect to the radius then they intersect at approximately diametrically opposite points. The chief disadvantage of the semi-circular focussing principle is that there is only one-dimensional focussing, i.e. in the plane of the circles. In 1946 a device was developed which combined many of the advantages of the one-dimensional focussing with those of the two-dimensional helical or lens focussing. This was the double focussing spectrometer<sup>7</sup>.

Another flat spectrometer developed was the third order focussing spectrometer which corrected for the spherical aberration characteristics of the homogeneous magnetic field used in semi-circular focussing by shaping the magnetic field<sup>8,9</sup>. Still others include those arranging a focussing "prism" field where the source and detector are outside the magnetic field or a sector field with inhomogeneous fields and shaped pole pieces<sup>10</sup>.

The helical or lens-type spectrometer was first suggested

by Kapitza in 1924 (referred to by Tricker in reference 12), the electron focussing properties of short and long coils having been known for some time. Busch<sup>11</sup> was the first to point out the close analogy between light and electron optics if one replaces the optical lens by a magnetic "lens".

If electrons are emitted from a source, placed on the axis of an axial symmetric field, at some angle (other than  $0^\circ$  or  $90^\circ$ ) with respect to this axis, they will follow helical trajectories and return to the axis at some point P. (Fig. 3) Of course, the angle of emission cannot be so great as to carry the electron out of the influence of the magnetic field. Due to spherical aberration the maximum convergence of these trajectories occurs, not on the axis, at P, but at some ring of points concentric with the axis, i.e. at the "ring focus", F. This is typical of all lens-type spectrometers whether the field is homogeneous (solenoidal spectrometers) or inhomogeneous (long and thin lens spectrometers).

The first attempts to use a magnetic lens for beta-ray spectroscopy were made by Tricker<sup>12</sup> who used a long uniform field, i.e. a solenoidal spectrometer, and Klemperer<sup>13</sup> who used a short field. These early instruments could not compare with the performance of the flat spectrometers because no serious efforts were made to improve their performance. The potentialities of these helical instruments were not fully realized until the early forties when Witcher<sup>14</sup> developed the solenoidal spectrometer and Deutsch et al.<sup>15,16</sup>, the short

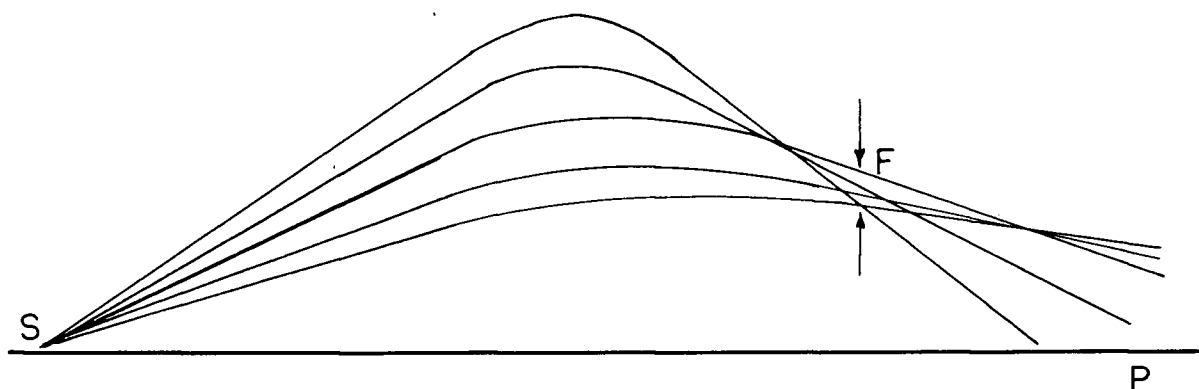


Fig. 3. Helical Spectrometer Electron Trajectories

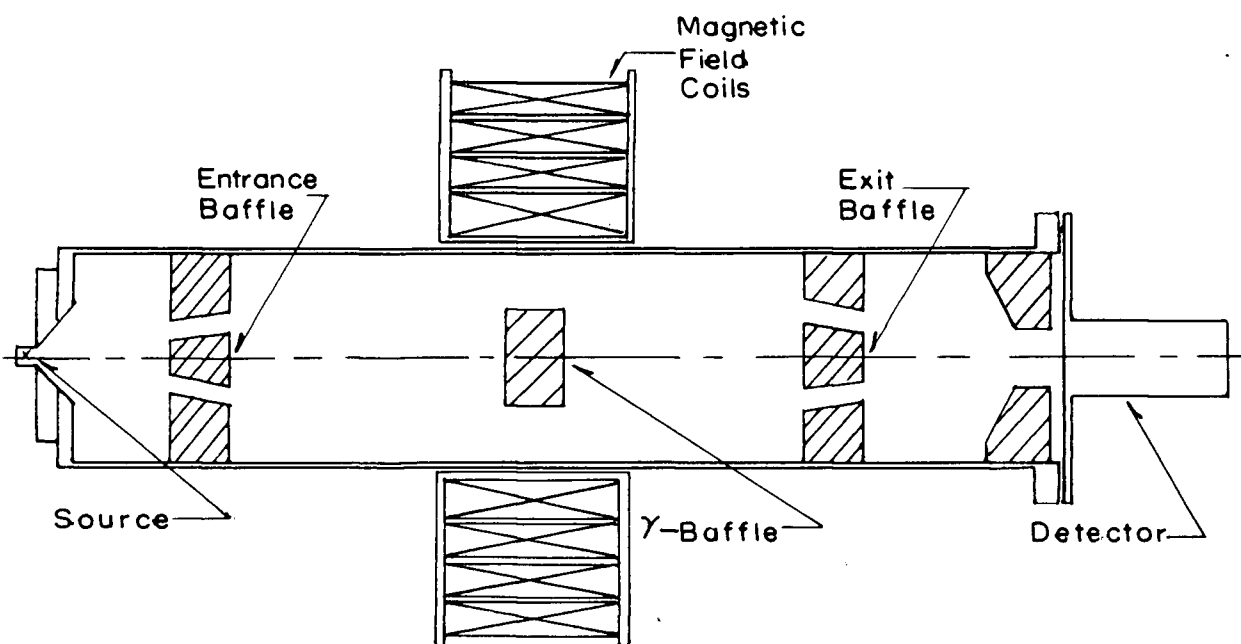


Fig. 4. Unmodified Thin-Lens Spectrometer



lens spectrometer. The short lens used by Deutsch played the predominant role in the accumulation of data which followed the successful introduction of the lens method. This is not meant to imply that the short or thin lens gives the best performance. It is flexible in its performance and easy to construct with source and detector out of the magnetic field, an important feature in angular correlation work and in detector shielding. Also it is relatively inexpensive to construct and requires less electric power to operate than do most other magnetic spectrometers. However, it has inherently large spherical aberration.

The characteristics of other helical spectrometers may be mentioned. The solenoidal spectrometer had the advantages of a uniform magnetic field, so that electron trajectories may be calculated rigorously, of easy adjustment and of relatively low sensitivity to outside fields. However, they have large power requirements. Still better performance is obtainable by field forming. This technique is employed in the "intermediate image" spectrometer where the electrons pass through two adjacent lens fields, the first focussing in the normal way to a ringfocus and the second reversing the process by having a field the mirror image of the first. Thus the final result is an axial image. Another example is the long lens spectrometer which theoretically has significantly less spherical aberration than the thin lens spectrometer.

The chief advantages and disadvantages of the thin lens

spectrometer have already been mentioned and it is this type of spectrometer which is in use in this laboratory. A simple diagram is shown in Figure 4. Its operation is clear from the previous discussion. The gamma-baffle is to protect the counter from direct radiation and the other baffles are for electron selection. Only those electrons which pass through the entrance and exit baffles are counted. Since the path of the electron depends on the magnetic field and electron momentum, one may, by keeping the radius of curvature constant and varying B, determine the relative intensity distribution of the momentum of the electrons being emitted by the source and collected by the detector.

Some important spectrometer parameters.

It is convenient in the discussion of a spectrometer's performance and for comparison with other spectrometers to define the two parameters already mentioned, transmission and resolving power, and several others in precise mathematical terms.

Transmission: The transmission, T, is a measure of the collecting power of the spectrometer and is expressed as a percentage. T is the percentage of electrons emitted by the source that reach the detector and are counted when the instrument is adjusted to focus these electrons, i.e. the fraction of the solid angle at the source "seen" by the detector. Related to T is the gathering power,  $\omega$ , defined

as the ratio of the solid-acceptance angle,  $\Omega$ , to the total solid angle. It is defined by the entrance baffles.

$$\omega = \frac{\Omega}{4\pi} \quad \text{Of course, } T \leq \omega$$

Resolution: The resolution,  $R$ , is a measure of the selective power of the detector system. If monoenergetic electrons are emitted by the source, as in the case of conversion electrons, they will not appear in the spectrum as lines but rather as peaks of finite width. This is caused by scattering, finite source and baffle size and the inherent spherical aberration of the focussing field, all of which prohibit a "point" (or ring of points) focus which is required for true spectrum lines. The resolution,  $R$ , is defined as a percentage by the equation:

$$R = \frac{\Delta(B\rho)}{B\rho}$$

where  $B\rho$  is the magnetic stiffness of the focussed electrons

$\Delta(B\rho)$  is the peak width at half intensity.

Dispersion: Dispersion,  $D$ , as the name implies, is a measure of the ability of the instrument to separate adjacent energies. Thus we see for an instrument to be of any value the dispersion or line separation must be greater than the line or peak width. It is defined as

$$D = \frac{dx}{d(B\rho)}$$

where  $x$  is the co-ordinate of the focus.

A consideration of the two parameters, transmission and resolution, shows that they are, to a certain extent, mutually conflicting. If one improves the transmission by increasing the source size or by opening the entrance slot, the resolving power decreases. The ratio of transmission to resolution,  $\frac{T}{R}$ , is a good measure of the quality of a spectrometer and is used extensively in the comparison of spectrometers. It is referred to as "the Figure of Merit".

## 11. THE DEVELOPMENT OF THE THIN-LENS SPECTROMETER

The first major contributions to the theory and construction of thin-lens spectrometers were made by Deutsch et al.<sup>16</sup>. They calculated the electron trajectories using the procedure of Busch<sup>11</sup> and analysed the spherical aberration effect theoretically and experimentally. With source and detector on the axis of the magnetic field they varied parameters such as source size, emergent angles, etc. They used a baffling system to define the electron path, thus determining the resolution and transmission of the spectrometer. Other baffles were used to stop direct gamma-rays from reaching the counter and to reduce counts due to secondary electrons scattered from baffles and from the vacuum chamber walls. Also by using a spiral baffle they were able to distinguish between positrons and negatrons. It is important to note that collection by means of a geiger counter was made on the axis. This limited the practical transmission to small values, since only in these circumstances was the axial "image" small enough to be handled conveniently. They also observed that good alignment of the magnetic axis and source-detector axis was necessary for optimum focussing and thus for best figure of merit.

As can be seen from Figure 3, a calculation of the electron trajectories shows that the envelope of mono-energetic electrons emitted by the entrance baffle has, after

passing through the field, its point of maximum convergence not on the axis but on a ring of points circumscribing the axis. This fact led several workers<sup>17,18,19,20</sup> to introduce an annular slit at the ring focus. This improved the Figure of Merit by a factor of 2. Due to the divergence of the electron envelope past the ring focus, an axial detector must be fairly large to collect all the electrons and hence is subject to large background noise or if it is made smaller to operate at lower background it causes a loss in transmission. A realization of this fact led J.A.L. Thompson (unpublished) of this laboratory to investigate the collection of electrons at the ring focus.

Thompson's detector consisted of a ring of anthracene scintillation crystals "cemented" with high viscosity silicone oil into a groove on the open lip of a lucite "light-cone". The light cone was optically coupled, using the same oil, to a photomultiplier tube.

Various detector systems were tried with a view to obtaining the best signal-to-noise ratio possible. The system described by K.C. Mann and F.A. Payne<sup>21</sup> and shown in Figure 5 being one of the most recent. It is this detector system, with some minor alterations, which is in use in this laboratory at the present time. The present detector system will be described in detail in a later section.

While the detector used by Mann and Payne<sup>21</sup> was considerably further away from the magnet coils than the source

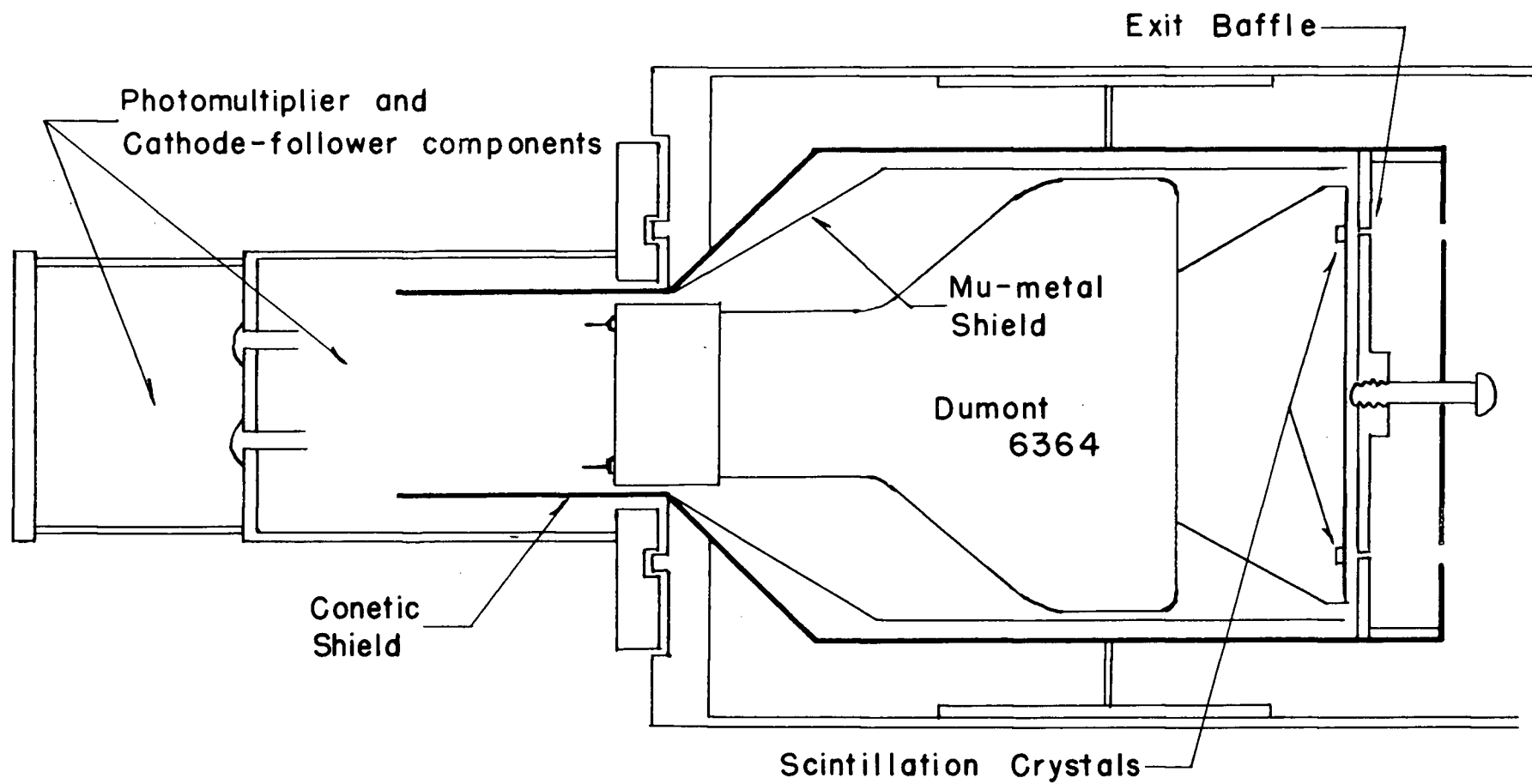


Fig. 5. Detector Assembly of Mann and Payne

it still lay within a residual magnetic field, which affected the performance of the photo-tube at high magnet currents. The photo-tube was shielded from these fields by placing the entire detector system (lucite and all) in a Conetic shield and by placing a Mu-metal shield around the photo-tube itself. It was found that this arrangement gave sufficient protection to leave the photo-tube output unaffected by the magnetic field for electron momenta less than 4,000 gauss-cm. However, above this momentum it was found that the greater focussing field began to reduce the photomultiplier output pulse.

Figure 6 shows the relative positions of source, magnet and detector, of the entrance and exit baffles and of the source centering controls used by Mann and Payne<sup>21</sup>. The entrance baffling system was mounted rigidly to the source holder which was mounted on a centering mechanism capable of moving the source to any desired position in a plane perpendicular to the magnetic field axis. This was found to be absolutely necessary, particularly when the baffles were chosen for optimum resolution, since otherwise the circular ring focus of the electron beam was not necessarily concentric with the annular exit slot. Before centering the source, the spectrometer was aligned in the center of the magnet as well as possible by visual observation. Even after source centering it was unlikely that the source-detector and magnetic axes were coincident, since the centering mechanism did not give the required number of degrees of freedom.



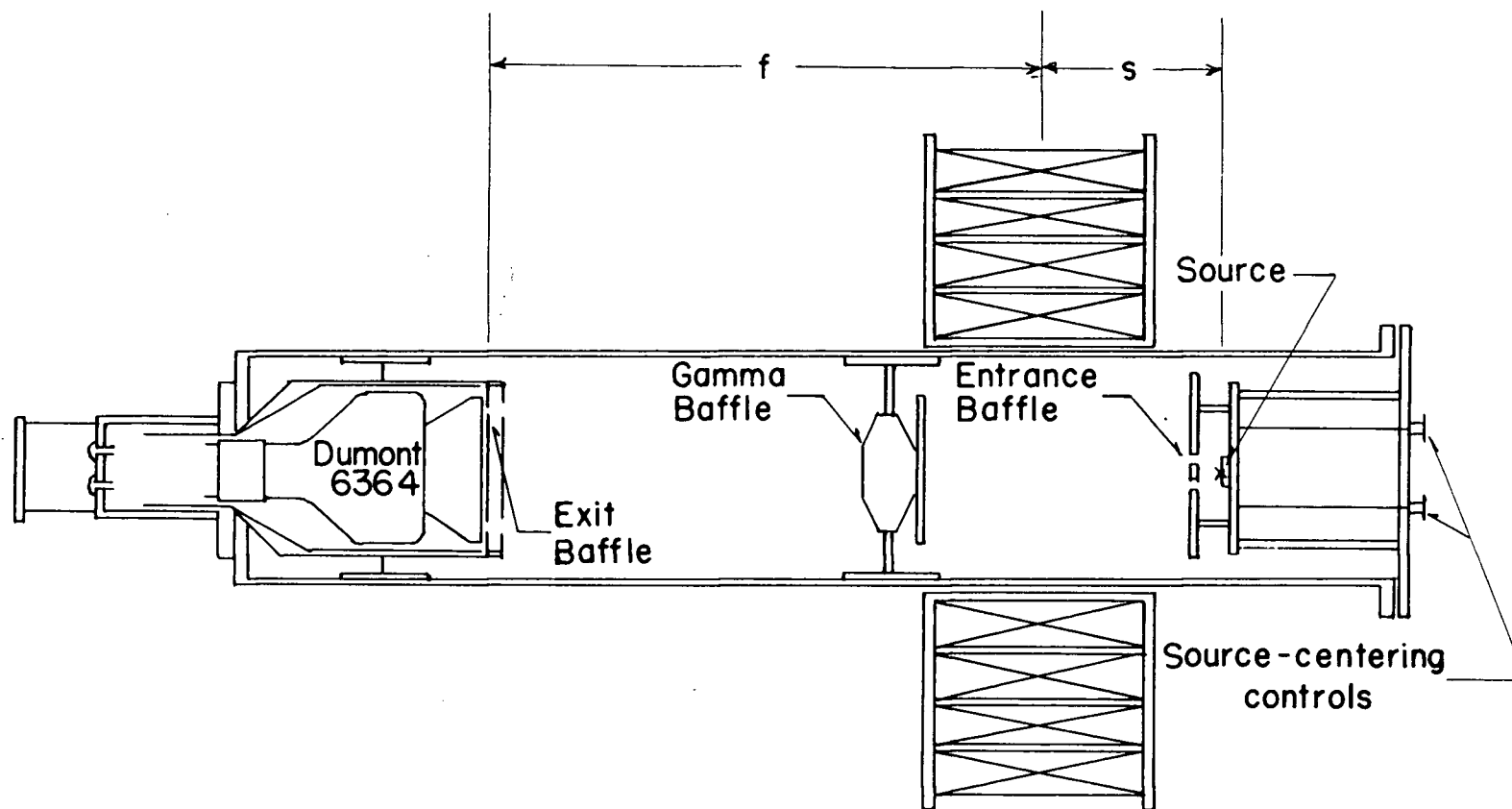


Fig. 6. Modified Thin-Lens Spectrometer

They investigated the performance of this instrument using a constant source-detector distance of 69.7 cm.; entrance baffles giving gathering powers of 0.7, 1.1 to 1.6%, the tangent of the mean angle of each trajectory envelope being .4, .385 or .352; ring focus detection by means of a 5.15 cm. mean radius circle of anthracene scintillation crystals and a  $\text{Cs}^{137}$  source mounted on a thin aluminum backing. For each gathering power they obtained an optimum source to magnet-coil-center distance,  $S$ , by installing a large exit slot and observing the profile of the  $\text{Cs}^{137}$  conversion peak for different  $S$  positions. The optimum value of  $S$  was considered to be the one of the set which gave a peak profile having maximum transmission and best resolution. (The two occurred simultaneously.) They then matched the annular exit slot with the annular entrance slot by reducing the exit slot width until the transmission started to drop. Each reduction in exit slot width before the transmission started to decline improved the resolution. Any further reduction did not improve the resolution but did cut down the transmission. The baffles were matched when maximum transmission and minimum resolution were obtained.

A comparison of the performance of some helical spectrometers was tabulated and that table is reprinted here:

TABLE I

Comparison of some high-performance helical spectrometers.

Type	Iron	(%)	R(%)	$\left(\frac{\omega}{R}\right) \times 100$
Solenoidal	No	2	0.4	500
Intermediate image	No	4.5	1.6	280
Long lens	Yes	6.3	2.4	262
Solenoidal	Yes	3	1.2	250
Long lens	Yes	2.7	1.3	208
Intermediate image	Yes	8	4	200
Intermediate image	Yes	10	5.5	180
Long lens	No	11	9	122
Thin lens	No	1.6	1.37	118

$\frac{\omega}{R} \times 100$  represents a rough figure of merit.

The modified spectrometer described above has certain limitations.

1) Magnetic Shielding. The source-detector distance is small enough to cause the detector assembly to lie in a residual focussing field. At sufficiently high magnet currents, this field adversely affects the photomultiplier output. Calculations show that an increase of 20 cm. in the magnet-detector distance would practically eliminate the shielding problem.

2) Centering and Alignment. It has been found that source centering is very critical. There is evidence that centering by source movement only, produces an "optimum" for any relative position of source-detector and magnetic axes. However, if these two axes are not coincident, this "optimum" may not be the best attainable. This condition conceivably

could be improved if a method of bringing the two axes into coincidence were adopted.

3) Source Position. In the modified spectrometer the source is placed 11.6 cms. inside the end of the vacuum chamber. The walls of the chamber and the source centering mechanism behind the source prohibit one from modifying the end plate for angular correlation work. A simpler source holder which places the source at the end of the chamber would permit the possible use of the spectrometer for angular correlation work.

4) A minor inconvenience is the necessity of disturbing the source to reach the detector.

### III. PRESENT INVESTIGATION

#### A. INSTRUMENTATION

The present investigation was carried out on a spectrometer similar to the one used by Mann and Payne. The major differences in the two spectrometers are:

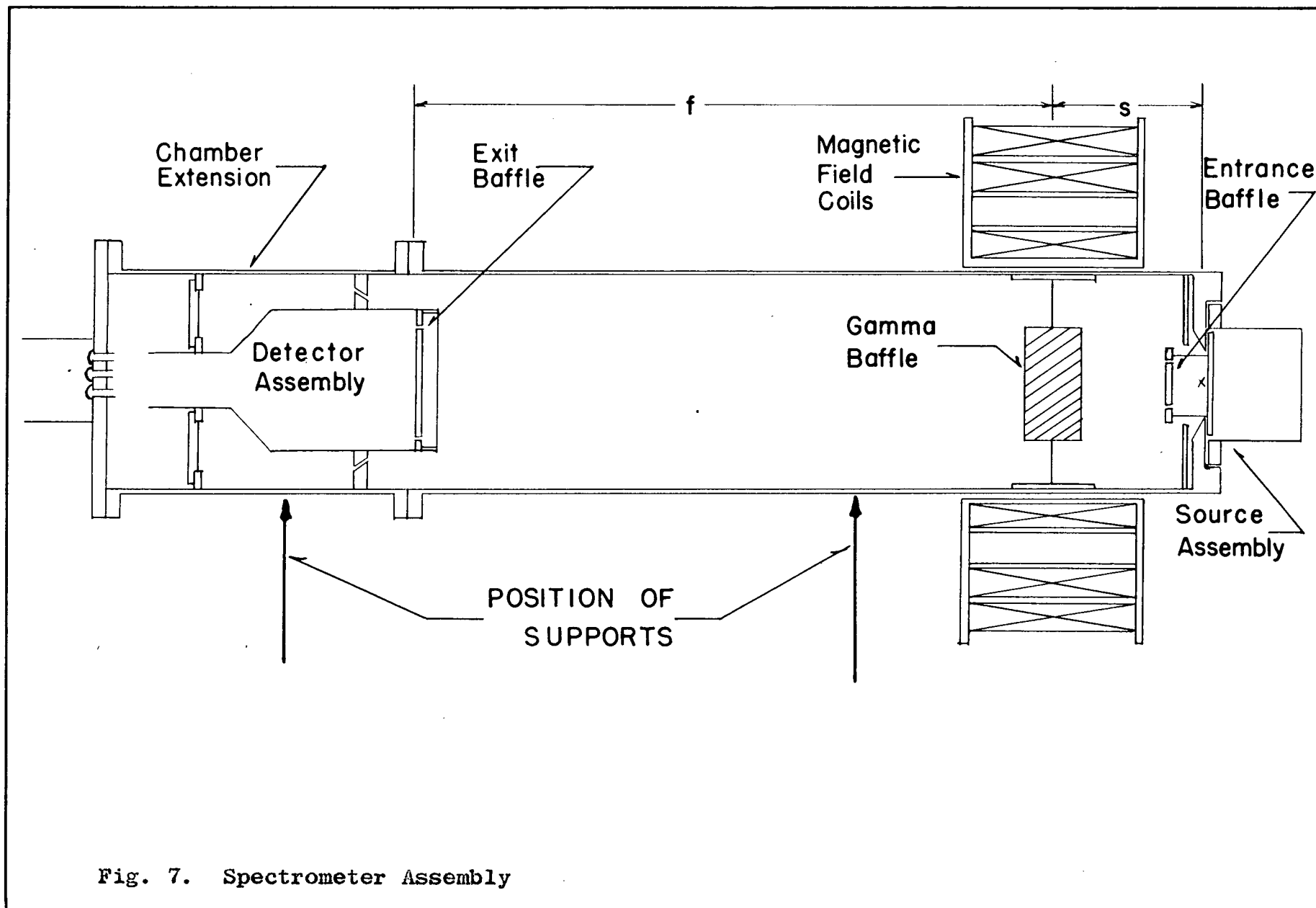
1) The magnetic field is formed by three sets of windings instead of four. (The innermost but one winding had, sometime before, shorted to the case.) Thus the field strength is correspondingly smaller for a given magnet current.

2) The vacuum chamber has been extended by a cylinder of brass 38 cms. in length and of the same diameter as the original chamber. This extension, shown in Figure 7, houses the detector assembly.

3) The end of the chamber which housed the source now holds the detector and vice versa. Also the source assembly has been constructed so that the source lies in the plane of the end of the chamber (Fig. 8).

4) A centering mechanism has been introduced so that accurate axial alignment can be made.

The source holder, the entrance baffle and their means of attachment to the chamber are shown in Figure 8. The entrance baffle is attached in a fixed position to a plate which in turn is fixed to the end of the chamber. The source is attached to this plate so that it can be positioned on the



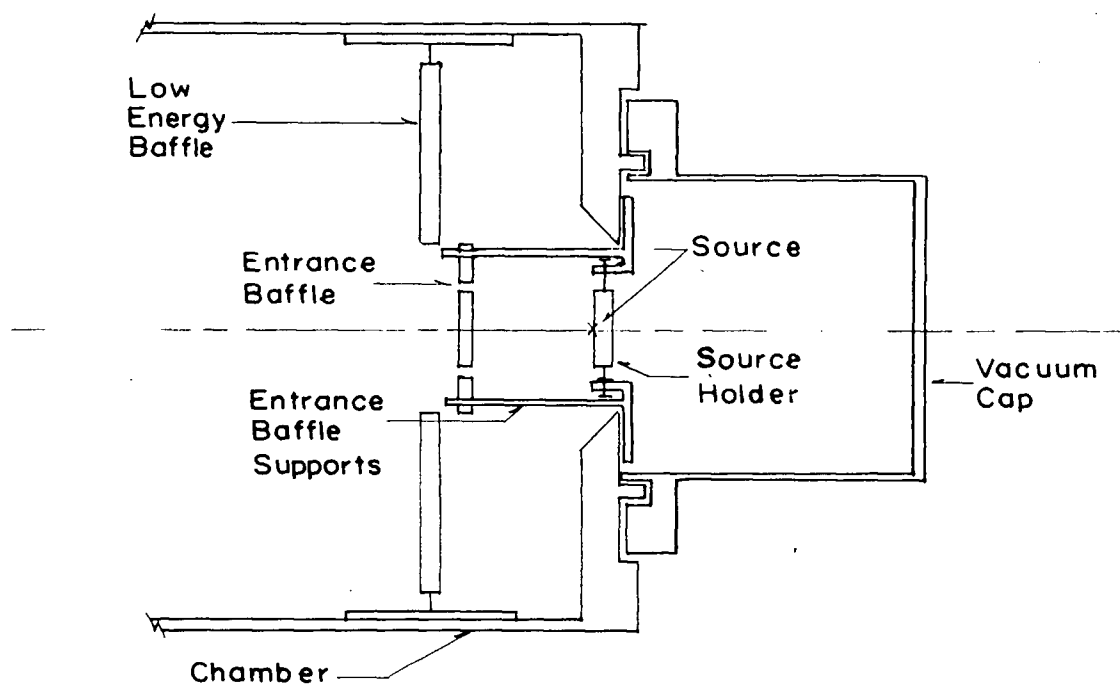


**Fig. 8. The Source Assembly**

central axis of the entrance baffle. In this way, the source or entrance baffle may be replaced without materially disturbing the assembly alignment. Also this assembly allows the source to be removed easily and exposes it for possible angular correlation work. In addition, Figure 8 shows a "low energy" baffle. This baffle protects the detector from any low energy electrons which might otherwise pass outside the entrance baffle and be focussed.

The end of the chamber containing the detector assembly is shown in Figure 9. The electrons, after travelling through the annular slot in the face of the Conetic shield, pass through the exit baffle and impinge upon anthracene crystals placed immediately behind. The exit baffle defines the ring focus which has a mean radius of 5.15 cms. The scintillation crystals are embedded in the face of a lucite cone with the aid of a silicone gel and the cone is coupled to the photo-sensitive face of a photomultiplier tube by silicone oil. This cone, and hence the crystals, is kept in place by a bakelite ring and a screw. The bakelite ring surrounds the base of the cone and is cemented to the photo-tube face. The screw passes through the face of the Conetic shield and screws through the exit baffle. The screw, by pushing against the face of the lucite cone, forces the cone against the photo-tube and forces the photo-tube into the base of the Mu-metal shield. Since the Mu-metal shield is fixed with respect to the Conetic shield and since the exit baffle is



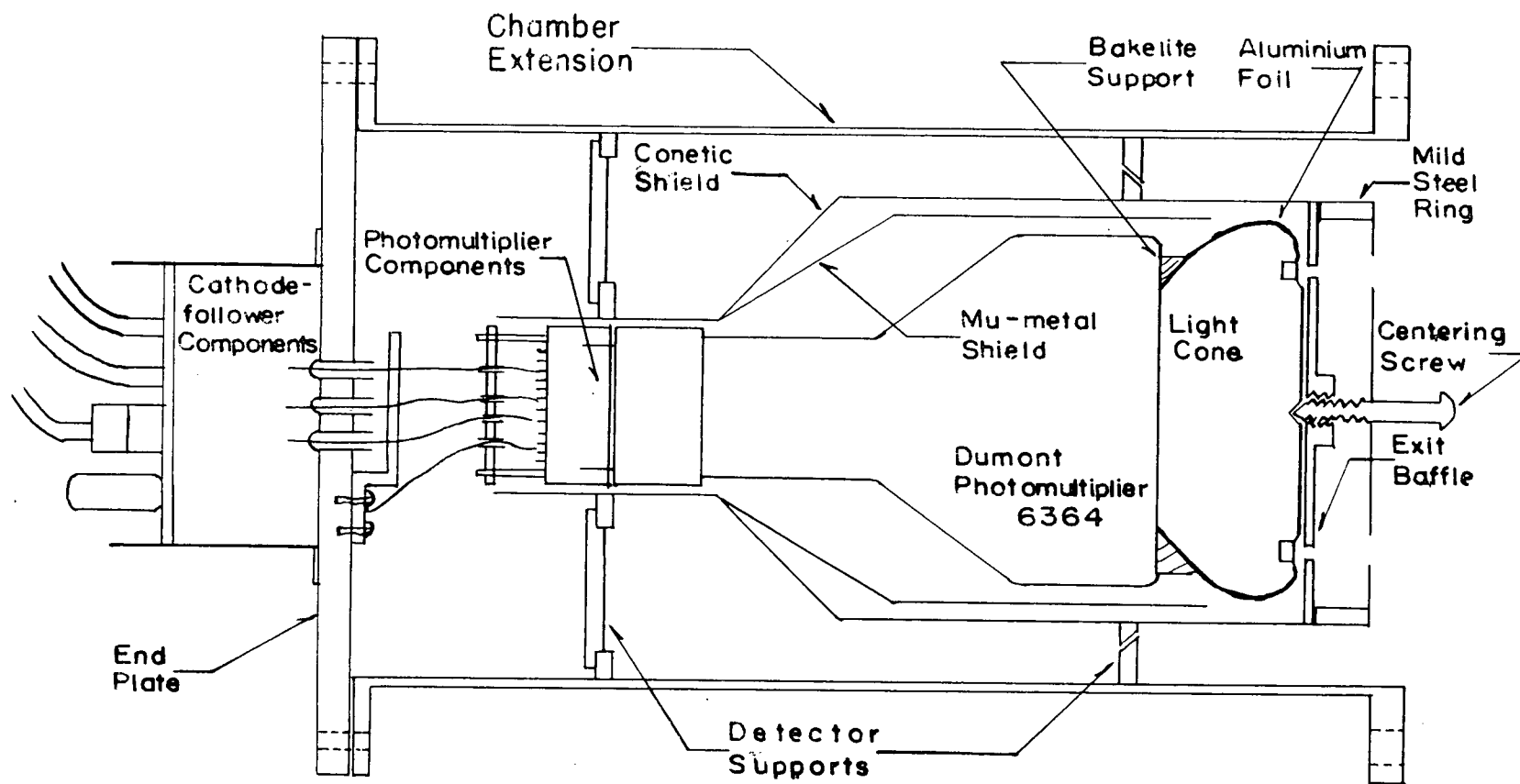


Fig. 9. The Detector Assembly

attached to the face of the Conetic shield by a mild steel cap, the whole assembly is fixed with respect to the Conetic shield. The crystals therefore are always immediately behind the exit annular slot. Finally, by means of ring supports on the inside of the chamber and on the outside of the Conetic shield, the Conetic shield is placed in a fixed position with respect to the chamber. This position is approximately in the center of the chamber and is always reproducible.

The Conetic shield was obtained from Perfection Mica Company, Chicago, Ill. Inside this shield and surrounding the photo-tube is a Mu-metal shield used to diminish the effect of low fields which penetrate the Conetic cores. The photomultiplier tube used is a Dumont 6364 which has a 5" diameter photosensitive cathode. It was selected from the three tubes available because it had the best signal-to-noise ratio. Normalizing the signal-to-noise ratio of the photo-tube used to 1, the corresponding signal-to-noise ratios of the two remaining photo-tubes were found to be .74 and .35. Finally, the sides of the lucite cone are short and were machined in the form of a section of a logarithmic spiral. The sides and front face (except for the crystal area) are covered with aluminum foil so as to minimize photon loss through the sides and end of the cone.

Each baffling system consists of two baffles, an inner and an outer. The inner baffle is attached by means of

"spider" legs (as shown in Fig. 10) to the outer baffle which is attached to a support fixed with respect to the vacuum chamber. These spider legs and baffles were carefully machined so that they fitted together exactly and so that different permutations of baffles could be made without requiring adjustments to the system. Entrance baffles were machined to give gathering powers of 1.5%, 1.1% and 0.7% at each of three mean admission angles. The tangents of these angles are .400, .388 and .353. Sets of exit baffles were machined to provide variation of the exit slot width by .25 mm. steps from 2.25 mm. to 4 mm.

With this design one may remove the source holder or detector assembly separately, so as to change baffles, source, crystals, etc., and replace the source holder or detector assembly with a minimum amount of readjustment. Because of the additional chamber length and the removal of the bulky source centering mechanism, the source-detector distance has been increased from 69.7 cms. as used by Mann and Payne to 100 cms.

The aim of the new centering technique is to obtain coincidence of the magnetic axis and the source-detector axis. The magnetic axis is fixed by the position of the magnet coils. The source-detector axis is fixed with respect to the vacuum chamber. Therefore, to obtain axial alignment and coincidence, it is necessary to be able to control the orientation of the chamber axis with respect to the magnetic axis, i.e. to

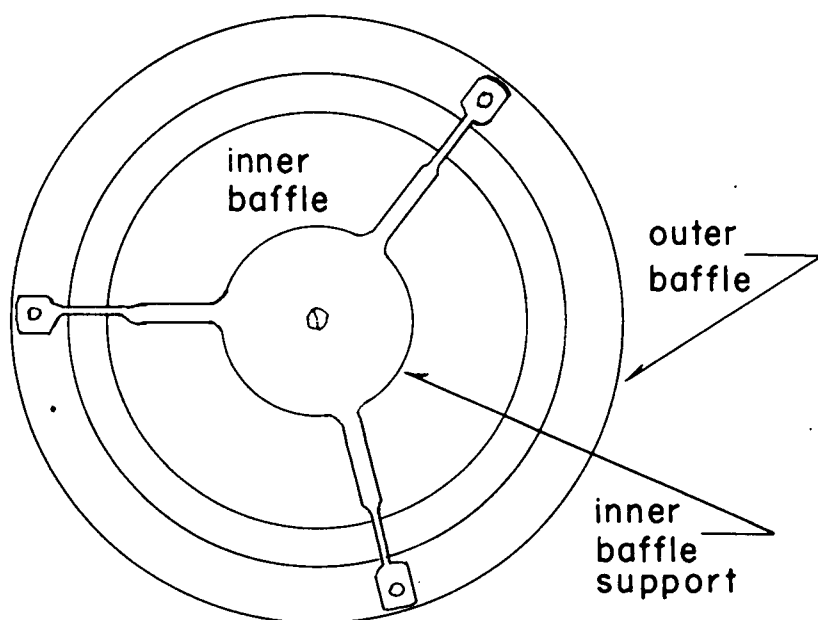


**Fig. 10. Sample Entrance Baffle**

be able to move the chamber laterally to any two dimensional grid position and to rotate it with respect to the fixed magnetic axis. The range of motion is, of course, limited by the size of the magnet coil opening. Finally, since the source-magnet distance is a parameter which cannot be constant, one must also be able to move the chamber longitudinally along its own axis.

To achieve this, the entire chamber is supported on two identical stands which were constructed to permit the required freedom of motion. An illustration of the stands used is shown in Figure 11. The two stands are placed on the spectrometer table in line with the magnet coil opening. The vacuum chamber rests on the corrugated rollers which permit motion of the chamber perpendicular to the magnet (i.e. a variation of  $S$ ). As can be seen from Figure 11, one can move the chamber horizontally by turning dial A, or vertically by turning dial B.

The circumference of the centering dials is divided into 10 divisions so that the relative motion of the chamber may be observed and so that the chamber may be returned to any set position. The motion of the chamber is determined by the motion of the screw threads attached to these dials. Since these screws have 25 threads to the inch, a rotation of one tenth of a revolution on the dial moves the chamber approximately .1 mm.

The axis of the magnet is placed parallel to the hori-

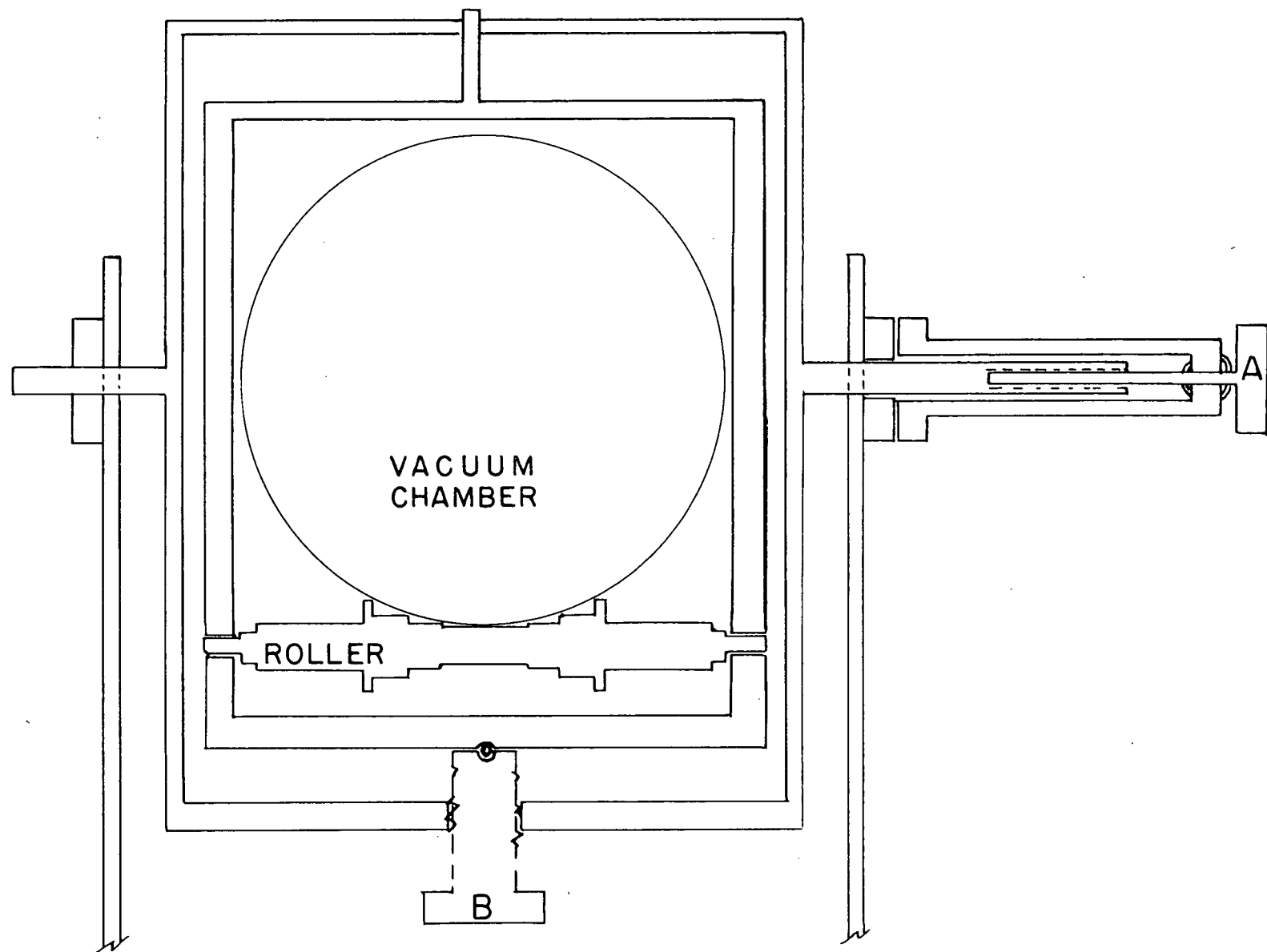


Fig. 11. Chamber Support

zontal component of the earth's magnetic field so that unfavourable defocussing effects due to the horizontal component of the earth's field are minimized. The vertical component is minimized by passing a direct current of 1.1 amperes through two compensating coils, contained in two horizontal planes above and below the spectrometer. They are 1.1 meters by 1.6 meters and the planes containing them are separated by 1 meter. The vacuum chamber lies midway between these two coils. A current of 1.1 amperes in these coils creates at the mid-point of the electron envelope, a magnetic field equal in magnitude but opposite in direction to that of the vertical component of the earth's field.

The d.c. magnet current is obtained from a 110 volt d.c. line. The current is regulated as follows. The current passes through the magnet coils, a bank of 6AS7 triodes and a standard  $0.03 \Omega$  resistor. The voltage developed across the standard resistor is balanced by a control chassis against the output of a potentiometer. Any error signal between these two provides a compensating voltage to the grids of the 6AS7's. Regulation in current to 1 part in  $10^4$  is achieved. By varying the potentiometer setting, the magnet current can be varied from 0 to 10 amperes (H - 0 to 5,000 gauss-cm.).

The photomultiplier H.T. is obtained by tapping the desired voltage from a bank of voltage reference tubes placed across the output of a regulated H.T. supply. Photomultiplier pulses pass through a cathode follower circuit mounted on the

vacuum chamber (see Fig. 9) into a commercial amplifier and bias discriminator whose constant height output pulses are counted by a scalar.



## B. EXPERIMENTAL TESTS

The chief purpose of the present investigation was to study the effect of the centering mechanism on the performance of the spectrometer. As has been stated, it is believed that for best performance the source-detector axis (fixed with respect to the vacuum chamber) should coincide with the axis of the magnetic field. Since the magnetic axis is fixed, the vacuum chamber must have sufficient freedom of motion to permit this axial alignment. It is necessary that the supports allow one to move the chamber axis anywhere within a small solid cone which has its apex at the magnet center and its axis along the magnetic axis. Also the supports must allow one to move the chamber axis onto the magnet center. It has been shown that the chamber supports permit this motion.

To calibrate the instrument, the profile and height of the 661.6 Kev. K-conversion peak of  $\text{Cs}^{137}$  was examined at various chamber positions. The optimum position for any set of entrance and exit baffles is that position giving minimum peak half-width and maximum peak height. Two  $\text{Cs}^{137}$  sources were studied. One had a source diameter of 2.4 mm., the other 1.6 mm. These were the two sources used by Mann and Payne in the calibration of their spectrometer thus permitting us to compare the performance of the two instruments.

A variety of methods of moving the chamber were considered with a view to obtaining a procedure whereby axial alignment

could be readily obtained. It is reasonable to assume that the magnetic axis is approximately normal to the magnet coil and that the source-detector axis is approximately coincident with the cylindrical axis of the vacuum chamber. Hence visual alignment of the chamber perpendicular to the magnet and visual centering of the chamber in the hole of the magnet coil should be a first approximation to axial alignment. Of course, after visual alignment the two axes are not likely to coincide exactly or even to lie in the same plane.

Assuming that the axes do not lie in the same plane after visual alignment and considering the optical analogy of a simple converging lens, an improved focussing condition should arise when the magnetic axis and the source-detector axis intersect at the magnet (lens) center. Presumably, this "intersection of axes" condition may be reached from an arbitrarily located source position by rotating the chamber, and hence the source-detector axis, about the position of the source until the best peak is obtained. This is not the ideal focusing condition since neither "object" nor "image" are located on the "optic" axis. After obtaining the optimum by rotation about the source, ideal axial alignment should then be reached if the chamber is rotated about the magnet center.

A possible alternative procedure would be to use a translational motion of the chamber to obtain an intersection of the two axes at the magnet center, as evidenced by maximum transmission and resolving power. Then, the final rotation

about this intersection point should put the axes in coincidence.

It is probable that all motions are interconnected, e.g. the optimum reached on a horizontal rotation may depend somewhat on the vertical setting. To take this possibility into account, repeat runs should form part of the setting up procedure.

After considerable experimentation with several combinations of entrance and exit baffles, a procedure was decided upon which appeared to give the optimum position. This procedure may be described by listing a sequence of steps to follow:

- 1) Select and install the desired entrance baffle.
- 2) Install some exit baffle. Preferably, the exit slot width should be larger than the slot width expected from previous experience.
- 3) Align the chamber visually in the center of the magnet opening and perpendicular to the plane of the magnet.
- 4) Obtain an optimum source-magnet distance by moving the chamber longitudinally until it is set at the position giving the best  $\text{Cs}^{137}$  conversion electron profile.
- 5) Rotate the chamber successively in a horizontal and vertical plane about the source position until an optimum profile is found. Repeat this procedure as many times as is necessary to obtain the same dial readings on two successive runs.

6) Rotate the chamber successively in a horizontal and vertical plane about the magnet center until the best profile is obtained.

7) Cut down the size of the exit slot until a match has been obtained. The exit baffle giving the best resolution without loss in transmission is considered to be the matching baffle for any particular entrance baffle.

While this procedure was fairly reliable, we found it necessary to check back and repeat after certain other steps had been completed. The optimum S position after visual alignment was sometimes found to be slightly different than the optimum after rotational alignment or after a better exit slot match had been made. Also the chamber position thought to be the optimum with one exit baffle was not always the optimum found after another baffle with smaller exit slot width had been installed.

The necessity to check the S position is to be expected since it is obtained in the beginning when the chamber is poorly aligned and the exit slot width is too large. Ideally, a repeat on the rotational alignment should not be necessary. It would be necessary if the position of the exit baffle with respect to the chamber is changed in the process of changing the baffle. It would also be necessary if the optimum position found with the large exit slot width is only approximate. After some experience it was concluded that the rotational procedure should be repeated because the optimum position

obtained with a large exit slot width is generally not the true optimum as determined with matching baffles.

We also found that, for the majority of runs, rotation about the magnet center after rotation about the source did not give a noticeably better profile. Thus we concluded that, because of the finite size of the source and because of the small source-magnet distance, (approximately 18 cms.) the magnetic axis probably passed through the source area even after visual alignment only. Therefore, rotation of the chamber about the source was sufficient to align the axes satisfactorily. Conceivably with a smaller source or greater source-magnet distance (necessary if entrance baffles giving a smaller emergence angle were used) rotation about the magnet center would be necessary.

Initially, we thought that a translational motion, after visual alignment would give the same results as rotation about the source. However, when this method was tried, the results were far less satisfactory and so the method was abandoned.

Changes in chamber position required to produce significantly poorer performance were much smaller than originally expected. Figure 12 shows the change in peak profile produced by a horizontal translation. It shows that a misalignment of 0.25 mm. has a noticeable effect on the peak profile and that a misalignment of 0.5 mm. is intolerable. This set of curves was taken with a poor baffle match, before the chamber had

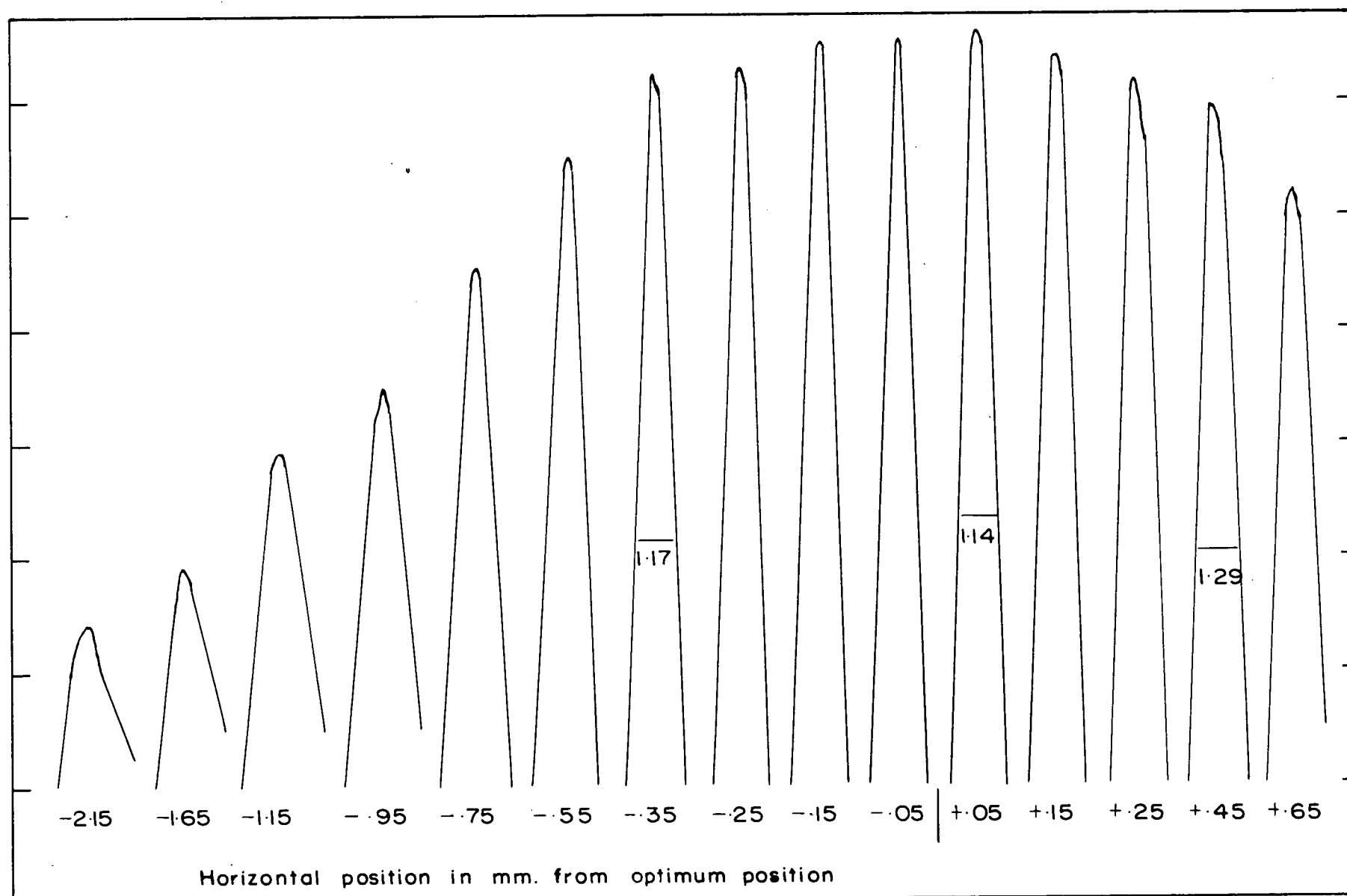


Fig. 12. Variation of Peak Shape with Chamber Position

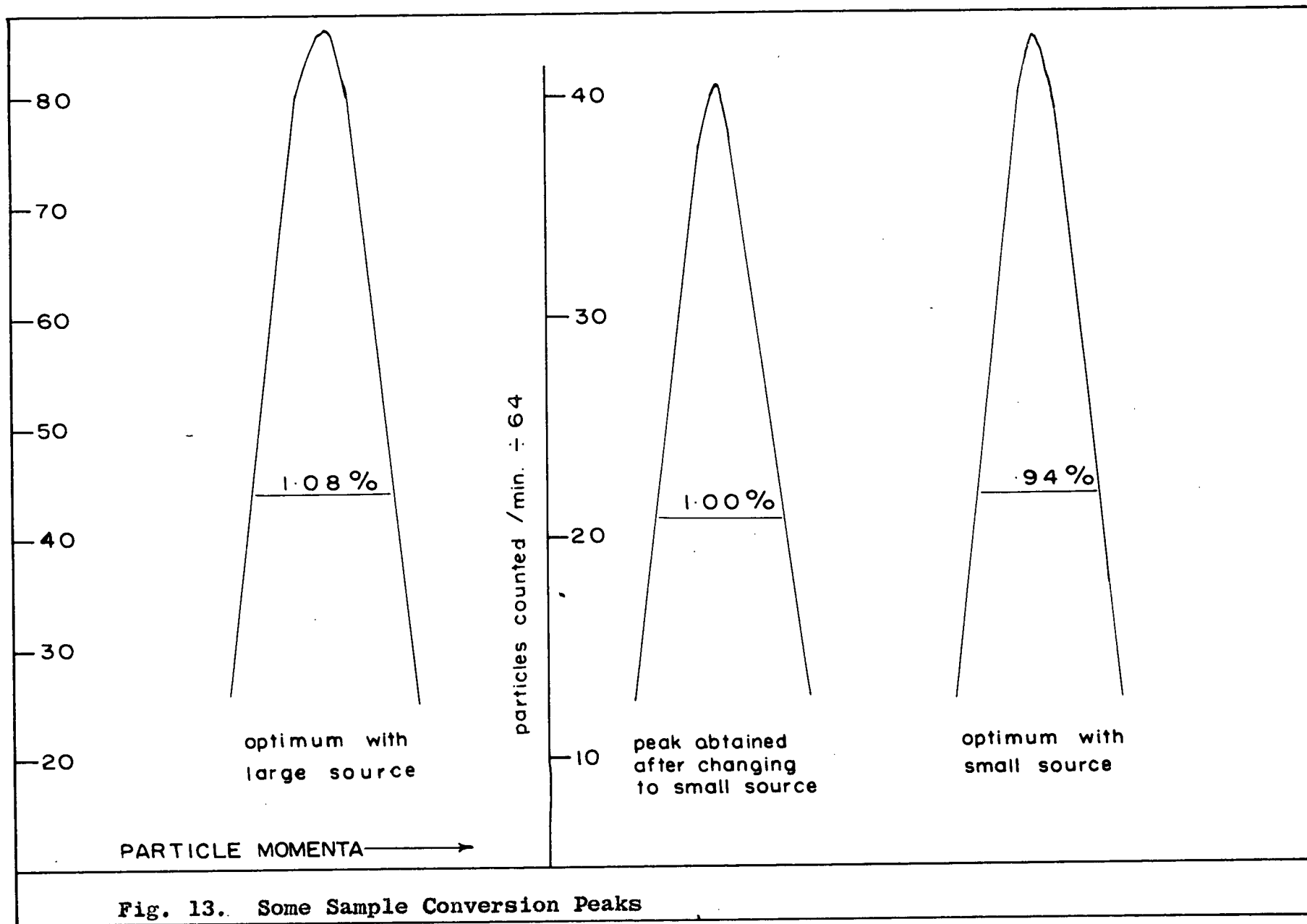
been properly centered and while using the less sensitive 2.4 mm. diameter source. After good alignment with the smaller source, a rotational motion away from the optimum caused by moving the inner support by 1.0 mm. and the outer support by 2.5 mm. was found to have a noticeable effect. This source rotation is equivalent to changing the angle between the source-detector axis and the magnetic axis by  $0^{\circ}09'$ . Unfortunately, this extreme sensitivity caused us considerable trouble for, not anticipating such sensitivity, the chamber supports lacked the rigidity required for good stability. Backlash in the screw threads also contributed to our experimental difficulties.

One other point should be mentioned. We had hoped, in the design of the source and detector assemblies, that the exit baffle, crystals, etc. and the entrance baffle and source could be changed without requiring further centering. The detector system may be removed and replaced without disturbing the centering. However, it seems that any change in entrance baffles and certainly any change in source requires recentering. This is probably because the source assembly is much closer to the center of the magnetic field than the detector assembly and therefore its position is much more critical.

Using an entrance baffle giving a gathering power of .70% at a mean emission angle of arc-tangent 1.50 it was found that the optimum S position was 18 cms. With the large Cs<sup>137</sup>

source, a resolving power or half peak-height width of  $1.08 \pm .01\%$  was obtained. Mann and Payne, with their spectrometer, obtained 1.13% with similar entrance slot characteristics. The large source was then removed and the smaller one installed. Before further centering the resolution was observed to be 1.00%. After further centering the optimum position gave a resolving power of  $.94 \pm .01\%$ . Figure 13 shows a sample of the curves giving these results.





### C. CONCLUSION

It has been mentioned that rotation about the magnet center generally was not necessary. One might suspect that the present centering mechanism gives the same alignment as can be obtained by Mann and Payne. The difference is that they move the source to obtain an optimum position while our rotation about the source is equivalent to moving the detector. Since the source is much closer to the magnet than the detector, the probability of the source lying on the magnetic axis after visual alignment is considerably greater than the probability that the detector does. For this reason it is likely that rotation of the source-detector axis about the source gives axial alignment whereas positioning of the source does not.

A comparison of the rough figures of merit,  $\frac{\omega}{R} \times 100$ , obtained by Mann and Payne at different gathering powers, is made in Table II. Also the values we obtained with a gathering power of .70% are shown in parenthesis.

TABLE II

(%)	$(\frac{\omega}{R}) \times 100$	
	Large source	Small source
1.6	108	117
1.1	84	89
.7	64 (64)	64 (74)

Mann and Payne found that the rough figure of merit became

poorer as the entrance slot width was decreased. We believe this change in performance to be caused by two factors.

1) Misalignment of axes. This resulted in a non-circular ring focus at the detector which did not coincide exactly with the exit slot. This lack of coincidence would cause poorer performance at all gathering powers. It would become more serious as the gathering power was decreased because the smaller the entrance slot, the smaller the width of the electron envelope and hence the greater the adverse effect of a non-circular image on the resolution.

2) Finite source size. The source diameter was comparable to the entrance slot width. As a result a performance that would be poorer than for a point source is expected and in fact the deviation from the ideal point source performance will increase as the entrance baffle slot is decreased.

The results of Mann and Payne show that at large gathering powers the small source gives better performance than the large source. This is to be expected from the above argument. However, at a gathering power of .70% the performance was not improved by replacing the large source by the small one. This would indicate that at this gathering power the adverse effects due to misalignment were much more serious than those due to source size and so any advantage expected by smaller source size was lost. Our results seem to confirm this belief for, with better axial alignment, we did obtain better performance with the smaller source.

A more detailed study of the effects of the diameter of the source on the spectrometer performance is necessary before any quantitative answers can be given on the relative importance of these two effects.

The activity of the small source was measured by H.R. Schneider of this laboratory by comparison with a Cs<sup>137</sup> source which he carefully calibrated. It was found that the transmission obtained by Mann and Payne with a gathering power of 1.1% was .56%. Similarly, we found that with a gathering power of .70% our transmission was .24%. This represents a loss in theoretical transmission of 50% and 65% respectively. This result is difficult to understand and it results in a spectrometer performance considerably poorer than should be expected. As yet we have not found an explanation for this and it remains to check this effect, to explain it and, if possible, to correct it.

Two other recommendations for improvement might be made. Firstly, the supports were originally constructed without the rigidity necessary and with a large amount of backlash in the positioning screws. The most serious fault of the supports is their lack of rigidity which meant that during the experimentation it was very difficult to return to the position selected as the optimum, after it had been passed. An improved support design might involve a jack supporting the chamber from below rather than from the sides and having sufficient rigidity to prohibit even minute motions under the

frictional forces involved in moving the chamber. Finally, if screw threads are used for moving the chamber they should be designed for a minimum amount of backlash.

The other recommendation is related to the compensating coils. Deutsch et al.<sup>16</sup> found that

"At low energies stray magnetic fields may be a serious source of trouble. A component of magnetic field perpendicular to the axis of only 0.01 gauss will displace the image by about 0.1 cm. with electrons of about 0.1 Mev. energy".

We found that with the desired current of 1.1 amperes in the compensating coils the vertical component of extraneous magnetic fields varied from 0 gauss along 75% of the electron's trajectory to approximately .05 gauss at the extreme ends of the trajectory. Calculations show that this extraneous magnetic field has negligible effect on the electron trajectories in the energy interval used in this experiment ( $> .6$  Mev.). However, for work in the low energy regions this magnetic field would result in poorer performance. New compensating coils to correct for the earth's field over the entire electron envelope are now being constructed and so the adverse effects due to the earth's field experienced at low energies will be eliminated.

BIBLIOGRAPHY

1. M. Goldhaber and G. Scharff-Goldhaber, Phys. Rev. 73, 1472 (1948).
2. M. Goldhaber and A.W. Sunyar, Phys. Rev. 83, 903 (1951).
3. E. Segre and A.C. Helmholtz, Rev. Mod. Phys. 21, 271 (1949).
4. M. Goldhaber and R.D. Hill, Rev. Mod. Phys. 24, 179 (1952).
5. v. Baeyer and Hahn, Phys. Z. 11, 488 (1910).
6. J. Danysz, Le Radium 9, 1 (1912) and 10, 4 (1913).
7. K. Siegbahn and N. Svartholm, Nature 157, 872 (1946).
8. F.M. Beiduk and E.J. Konopinski, R.S.I. 19, 594 (1948).
9. L.M. Langer and C.S. Cook, R.S.I. 19, 257 (1948).
10. H.O.W. Richardson, Proc. Phys. Soc. 59, 791 (1947).
11. v. H. Busch, Ann. Physik 81, 974 (1926).
12. R.A.R. Tricker, Proc. Camb. Phys. Soc. 22, 454 (1924).
13. O. Klemperer, Phil. Mag. 20, 545 (1935).
14. C.M. Witcher, Phys. Rev. 60, 32 (1941).
15. M. Deutsch, Phys. Rev. 59, 684A (1941).
16. M. Deutsch, L.G. Elliott and R.D. Evans, R.S.I. 15, 178 (1944).
17. S. Frankel, Phys. Rev. 73, 804A (1948).
18. J.W.M. DuMond, R.S.I. 20, 160 (1949).
19. J.M. Keller, E. Koenigsberg, A. Paskin, R.S.I. 21, 713 (1950).
20. W.W. Pratt, F.I. Boley, R.T. Nichols, R.S.I. 22, 92 (1951).
21. K.C. Mann, F.A. Payne, R.S.I. 30, 408 (1959).
22. I. Kaplan, Nuclear Physics, Addison Wesley.
23. K. Siegbahn, Beta- and Gamma-Ray Spectroscopy, North-Holland Publishing Company.
24. T.R. Gerholm, Handbuch der Physik, Vol. XXXIII.